Green Chemistry

Theobromine and Direct Arylation: A Sustainable and Scalable Solution to Minimize Aggregation Caused Quenching

Journal:	*Green Chemistry*
Manuscript ID	GC-COM-09-2019-003391.R1
Article Type:	Communication
Date Submitted by the Author:	02-Nov-2019
Complete List of Authors:	Huang, Yunping; University of Washington, Materials Science & Engineering Liu, Yun; University of Washington, Chemistry Sommerville, Parker; University of Washington, Chemistry Kaminsky, Werner; University of Washington, Chemistry Ginger, David; University of Washington, Department of Chemistry Luscombe, Christine; University of Washington, Materials Science & Engineering

Green chemistry and a natural product together create a cost-effective, safe and scalable solution to create luminophores with suppressed aggregation quenching in organic semiconductors.

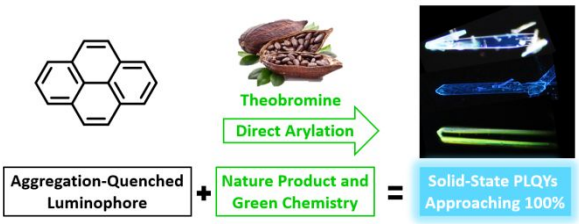

COMMUNICATION

Theobromine and Direct Arylation: A Sustainable and Scalable Solution to Minimize Aggregation Caused Quenching

Received 00th January 20xx,
Accepted 00th January 20xx

DOI: 10.1039/x0xx00000x

Yunping Huang,[a] Yun Liu, [b] Parker J. W. Sommerville, [b] Werner Kaminsky, [b] David S. Ginger [b] and Christine K. Luscombe* [a,b]

A green and scalable method to synthesize organic luminophores with minimal aggregation caused quenching (ACQ) is reported where direct arylation is used to attach alkylated theobromine moieties onto luminophores. The resulting compounds demonstrated high photoluminescence quantum yields (PLQYs) in solution and as aggregates. The minimized ACQ can be ascribed to the large dihedral angles that theobromine moieties introduce into these molecules, preventing π-π interaction between the luminophores. Furthermore, the large dihedral angles promote the formation of hybridized local and charge-transfer states in these molecules. Finally, amplified spontaneous emission measurements were performed to explore their potentials in lasers.

Aggregation caused quenching (ACQ) of fluorescence is commonly observed in organic luminophores.[1] While there are a number of reasons why ACQ can take place, in the case of organic luminophores with extended π conjugation, such as pyrene[1b] and perylene diimide,[2] the molecules can interact with each other *via* π orbital overlap and form non-fluorescent excimers. Aggregation causes non-radiative thermal decay to occur, dissipating energy into heat instead of light emission. This limits their efficiency in luminescent applications, such as organic light emitting diodes (OLEDs) and organic lasers (OLs).[1]

To date, numerous efforts have been invested into suppressing ACQ in organic luminophores including blending,[3] co-crystallization,[4] and covalently attaching functional moieties.[5] In this paper, we focus on advancing the chemical methods, whose products can be solution-processed, which is crucial for future scale-up and low-cost device fabrication.[6] Huang *et al.* suppressed ACQ by attaching bulky oligo-alkylfluorene moieties onto luminophores (**Fig. 1**).[7] Once installed, the fluorene modifiers were able to act as spacers, preventing luminophore aggregation and thus improving the solid-state photoluminescence quantum yields (PLQYs). Moreover, because the oligo-alkylfluorenes are conjugated, charge mobilities were maintained after modification, in sharp contrast to insulating spacers.[8] Tang *et al.* discovered that ACQ can be suppressed by attaching tetraphenylethene (TPE) onto luminophores triggering the mechanism of aggregation induced emission (AIE).[1b] Impressive results have been obtained by applying these types of materials to OLED and OL devices.

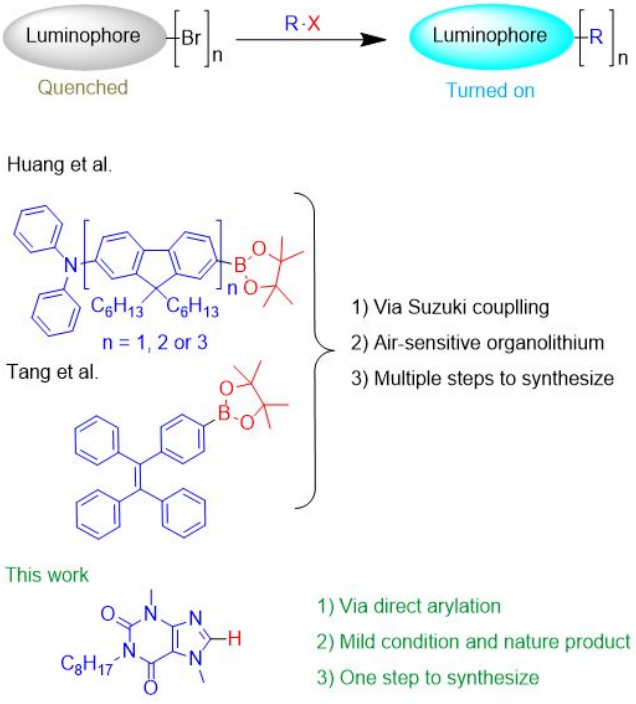

Fig. 1. Chemical modifications for organic luminophores to suppress ACQ.

[a] *Department of Materials Science & Engineering, University of Washington, Seattle, WA 98195.*
[b] *Department of Chemistry, University of Washington, Seattle, WA 98195.*
† Footnotes relating to the title and/or authors should appear here.
Electronic Supplementary Information (ESI) available: [details of any supplementary information available should be included here]. See DOI: 10.1039/x0xx00000x

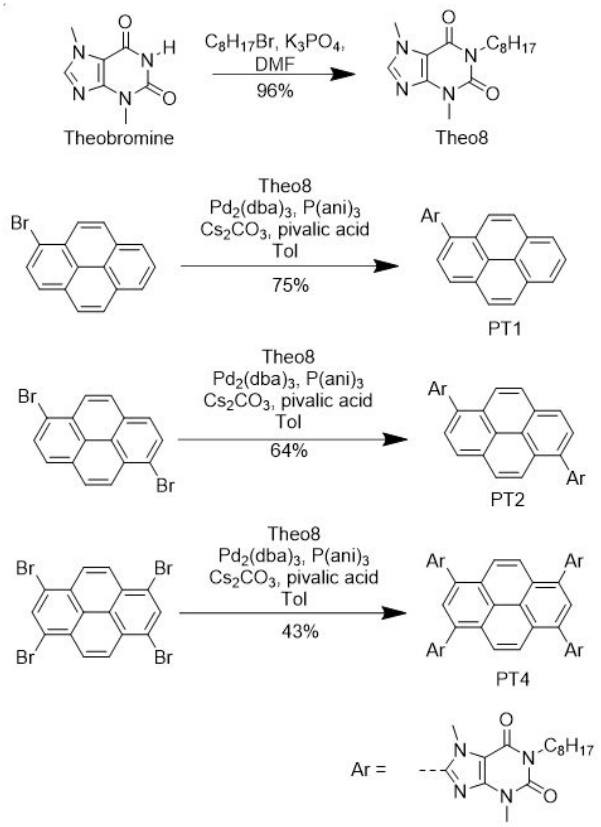

Scheme 1. Synthetic routes for **PT1**, **PT2** and **PT4**.

However, these methods bring up environmental concerns: they heavily rely on Suzuki coupling, which uses air-sensitive and explosive organolithium compounds to prepare boronic ester precursors.[9] Should these materials be prepared at a commercial scale, a method avoiding organolithium would substantially diminish workplace safety risks. Moreover, organolithium decreases the functional group tolerance in the synthesis, as it is strongly nucleophilic.

Direct arylation offers a green and atom-efficient method to form C-C bonds between aromatic building blocks. This direct formation of C-C bond allows us to bypass the extra step of precursor synthesis, where organolithiums are usually involved.[10] Therefore, the risks of fire and explosion are reduced, while cost and productivity are optimized. Moreover, direct arylation is compatible with large scale production.[11] Major pharmaceutical companies, such as Merck[12] and Pfizer,[13] are applying it into commercial production of medicines; flow chemistry has been successfully implemented enhancing productivity further.[14] Additionally, substrate compatibility is improved because of the absence of highly reactive intermediates. However, because the C-H bond on benzene has poor reactivity under the concerted metalation-deprotonation (CMD) mechanism,[15] it is not feasible to utilize direct arylation to attach oligofluorenes or TPE onto luminophores to minimize ACQ. A new moiety needs to be identified to pair with direct arylation to develop a green method to suppress ACQ.

In this paper, alkylated theobromine is introduced onto luminophores *via* direct arylation to suppress ACQ. The mild reaction conditions allow for wide functional group tolerance. In this strategy, theobromine has the following advantages: 1) it is a natural product originally from cacao plants that is now produced in industrial scale and thus readily available and inexpensive (see Table S1 for price comparison for starting materials on each route); 2) the imidazole C-H bond is highly reactive for direct arylation;[16] 3) the N-methyl group on imidazole will repulse the luminophore and induce a large dihedral angle, creating steric hinderance preventing the luminophores from interacting with each other; 4) the lactam group is applied widely in the design of organic semiconductors with high electronic performance and one can easily tune the processability of the final product by introducing different solubilizing chains onto it.[17] Pyrene was chosen as the luminophore to test the effectiveness of this method. Pyrene is highly fluorescent in solution but completely quenched in the solid state,[1b,18] making it a good candidate to examine our approach. Three theobromine-pyrene derivatives, with differing theobromine:pyrene ratios, were successfully synthesized and characterized.

Table. 1. Summary of photophysical details of **PT1**, **PT2** and **PT4** in 10^{-5} M chloroform and as thin films.

	Solution					Thin film				
	abs, max /nm	PL, max /nm	abs, onset / nm	Energy gap /eV	PLQY /%	abs, max /nm	PL, max /nm	abs, onset /nm	Energy gap /eV	PLQY /%
PT1	343	432	395	3.13	100	360	475	409	3.03	95
PT2	367	455	420	2.95	100	380	485	440	2.81	90
PT4	400	474	457	2.71	85	430	530	490	2.53	74

The synthetic route to **PT1**, **PT2** and **PT4** is straightforward, beginning with the N-alkylation of theobromine, as shown in **Scheme 1**. The relatively long octyl chains were introduced to increase the hydrophobicity of the final products, improving solubility in common solvents and enabling solution processing. The key intermediate **Theo8** was obtained in near quantitative yield. Subsequently, **Theo8** and pyrene was cross-coupled by direct arylation, forming **PT1**, **PT2**, and **PT4** with increasing equivalents of **Theo8**. Notably, these materials are made in just two steps from commercially available starting materials. In contrast, it would take two extra steps to synthesize these materials *via* Suzuki coupling: converting brominated pyrenes to pyrene boronic esters and brominating **Theo8**. Moreover, as for products with high functionalities such as **PT4**, their overall yields would be significantly reduced with each step added to the overall route due to relatively higher incomplete conversion of each synthetic step. As hypothesized, these three compounds show high PLQYs in both solid state and solution. Notably **PT1** shows the highest PLQYs of all, approaching 100% as thin films. Increasing the ratio of **Theo8** leads to a decrease of PLQYs as thin films, as shown in **Table 1**, consistent with the photoluminescence lifetime measurements in **Fig. S13**. Increasing the amount of **Theo8** in the molecules increases the size of their conjugated systems. This could lead to the increase in intermolecular π overlap in solid state, facilitating ACQ and thus lowering solid-state PLQYs.[1b] Notably, we spincoated thin films from **PT1**, **PT2** and **PT4** that have been stored under ambient conditions for over 1 year. The resultant films showed unvaried PLQYs compared to what they were 1 year ago (see **Fig. S14**).

Molecular packing has significant impacts on solid-state PLQYs.[19] We thus investigated how the molecules are arranged through single crystal X-ray diffraction (SCXRD) (**Fig. 2**). The dihedral angles between theobromine and pyrene are relatively large: 63°, 80° and 47° for **PT1**, **PT2** and **PT4** respectively. These large dihedral angles are caused by the steric repulsion between pyrene and the adjacent methyl group on theobromine. This steric repulsion forces these molecules to adopt a twisted conformation which prevents the π-π interaction between pyrene cores. **Fig. 2** shows the crystalline molecular arrangement of **PT1**, **PT2** and **PT4**. While each compound has different packing patterns, in all cases theobromine drives self-assembly, due to strong polar interactions between the lactam groups. Meanwhile, the pyrenes and alkyl chains are arranged according to the positioning of the theobromine moieties. As a result, adjacent pyrenes are separated from each other,

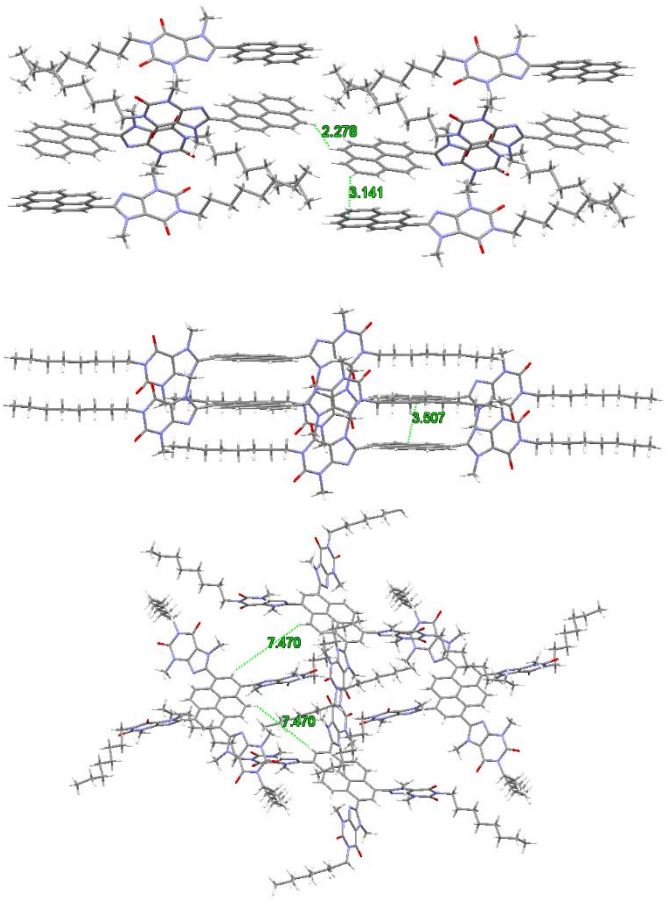

Fig. 2. Crystal structures of **PT1** (Top), **PT2** (middle) and **PT4** (bottom). H atoms, C atoms, N atoms and O atoms are labelled in white, grey, blue and red respectively. Distances between pyrenes moieties are given in green in the unit of Å.

effectively suppressing pyrene's ACQ in the solid state. To further confirm the efficacy of theobromine, we replaced the octyl on **PT1** with methyl and synthesized **PC** (**Scheme S1**). **PC** and **PT1** both demonstrated PLQYs around 95% as thin film, justifying theobromine is the origin for ACQ suppression.

As shown in **Table 1**, increasing the theobromine ratios leads to spectral redshifts in absorbance and emission, which implies that theobromine is conjugated to the luminophore it attaches to. This presents an apparent contradiction with the large dihedral angles observed by SCXRD, which would limit any such conjugation. It is proven feasible and widely applied using gas phase density function theory (DFT) simulations as close approximations for spincoated films considering their amorphous nature.[20] Molecular orbitals (MOs) were simulated based on B3LYP functional and 6-31g (d) basis set to investigate the apparent conjugation between theobromine and pyrene despite the large dihedral angles. Notably, there is an unusual distribution in the ground state (S_0) MOs of both **PT1** and **PT2**, as circled in **Fig. 3**. Despite the large dihedral angle between the pyrene and theobromine moieties, 63° for **PT1** and 80° for **PT2**, the orbital symmetries allow for MO overlap between the two moieties, intertwining around the single bond linkage. On the other hand, with a relatively smaller dihedral angle of 47°, the MOs of **PT4** extend through the molecule as commonly seen in other planar conjugated structures.

previous research has pointed out large dihedral angles are responsible for the formation of HLCT states and DFT simulations have shown that the energy curves of LE state and ICT state can crossover when its dihedral angle is sufficiently large.[22] Using our method, attaching theobromine moieties onto luminophores *via* direct arylation, one can easily introduce large dihedral angles into organic luminophores, thus inducing HLCT states in resulted materials.

As shown in **Table 1,** these pyrene-theobromine compounds possess high solid-state PLQYs and large Stokes shifts, which make them potential candidates for OL application.[23] We therefore studied their waveguiding properties in the solid state. When photopumping of the film is intense enough, spontaneously emitted photons are waveguided through the gain medium and amplified by stimulated emission, resulting in amplified spontaneous emission (ASE). To measure their ASE thresholds, a 375 nm laser beam was focused through a cylindrical lens into a stripe and used to photoexcited the thin film at a normal angle. Emission was collected from the edge of the film (see experiment set up in **Fig. S5**). **Fig.4a** shows fluence dependent emission spectra of a 90 nm thin film of **PT2** on a glass substrate. Its output spectrum significantly narrowed as the excitation fluence was raised above 20 μJ/cm². This spectral narrowing was accompanied by a sudden increase in output intensity vs. excitation fluence curve (**Fig. 4b)**. Taken together,

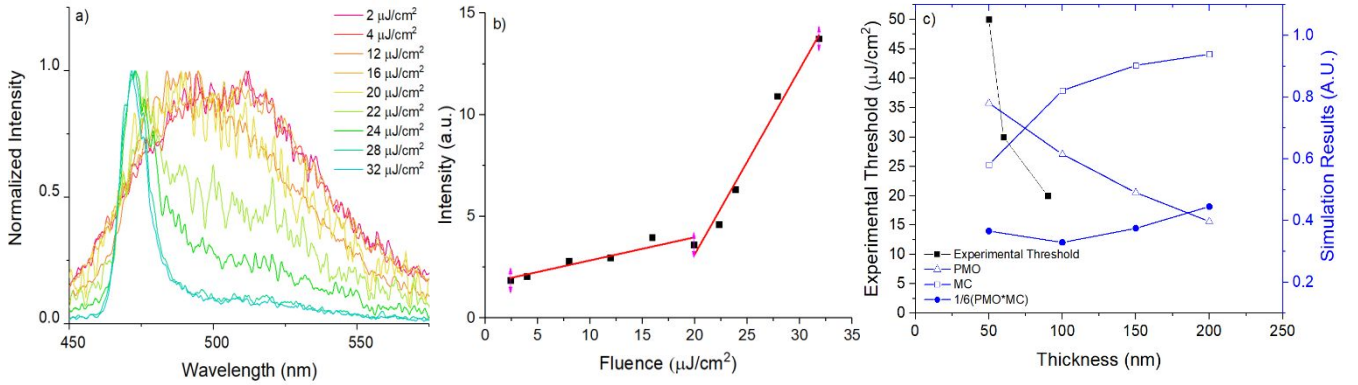

Fig. 4. a) Emission spectra of a 90 nm thick **PT2** film collected from the edge with increasing excitation fluence. b) Output intensity from the film edge as a function of the excitation fluence. c) Modelling of the pump mode overlap (PMO) and the mode confinement (MC), and their product (PMO*MC) scaled to fit in the same plot; experimental thresholds are plotted within for comparison.

In all three molecules, the MOs are spread out among the whole molecule in S_0, while in the first singlet excited state (S_1) the MOs are more localized onto the pyrene moieties. Therefore, their $S_0 \rightarrow S_1$ transitions contain a major part of locally excited (LE) transition of pyrene and a minor part of an intra-molecular charge transfer (ICT) transition from theobromine to pyrene. This implies that the S_1 MO is a hybridized local and charge-transfer excited (HLCT) state, as a result of LE state and ICT state inter-crossing.[21] HLCT states were further confirmed by solvatochromic experiments in **PT1**, **PT2** and **PT4**, as shown in **Fig. S3** and **S4**. HLCT states are crucial for the design of next-generation electroluminescence devices, where triplet excitons are converted into singlets excitons for fluorescence, breaking the theoretical limit of fluorescence devices.[21] Notably,

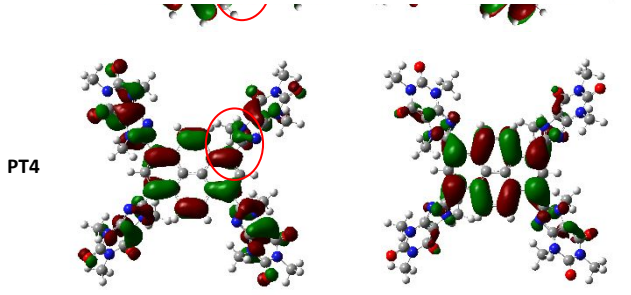

Fig. 3. Ground state and excited state MOs of **PT1**, **PT2** and **PT4**. The red circles highlight the differences of MOs at the pyrene-theobromine linkage.

Fig. 4a & **4b** indicate that the ASE threshold for **PT2** is 20 μJ/cm^2. In contrast, we did not observe ASE in **PT1** and **PT4** films of ~50 nm. Although emission was waveguided through the excitation area, PL emission intensity increased with pump intensity only in a linear fashion over several orders of magnitude (**Figure S6** & **S7**). We were not able to obtain smooth films of 90 nm from **PT1** and **PT4** because of the poor film-forming ability of small molecules in general.[24]

It is well-known that ASE threshold is dependent on film thickness,[25] and Bradley *et al.* calculated that a film thickness of 40 – 70 nm, depending on the compound, is prerequisite for ASE.[26] We did not observe ASE in the 50 nm films of **PT1** and **PT4**, likely because their thickness cut-offs are located at the upper end of 40 -70 nm range. We next investigated the theoretical thickness for lowest ASE threshold in **PT2** films based on the method reported by Anni *et al.,*[25a] using optical constants determined *via* a previously reported transfer matrix method (**Fig. S8**).[27] Briefly, we assume that the ASE threshold thickness dependence is governed by two factors: (1) the spatial overlap between the pump electric field and the guided mode (pump mode overlap, PMO in **Fig**. **4c**) and (2) the fraction of the guided mode that exists within the organic film (mode confinement, MC in **Fig. 4c**). We simulated the waveguiding of 0-1 emission, resolved from low-temperature PL measurements (**Fig. S9**) in a SiO_2-PT film-air slab waveguide. **Fig. 4c** shows MC and PMO in the waveguide as a function of film thickness. The ASE threshold, which is inversely proportional to the product of PMO and MC,[25]25[a] reached the minimum around 100 nm. This is consistent with our thickness dependent ASE measurement, where ASE thresholds of **PT2** decreased from 50, 30 to 20 μJ/cm^2 as the film thickness increased from 50, 60 to 90 nm. No ASE was observed in **PT2** film of 30 nm, in agreement with the calculation by Bradley *et al*.[26]

Conclusions

In this paper, we demonstrated that ACQ in pyrene can be effectively suppressed by modifying them with theobromine moieties *via* direct arylation. With this green and low-cost method, we synthesized three highly fluorescent pyrene-theobromine prototypes in two steps. SCXRD results showed the intermolecular π-π interaction between pyrenes were hindered due to the large dihedral angles introduced by theobromine moieties. As a result, ACQ was suppressed in these compounds and they are highly emissive both in solution and as solid. In addition, large dihedral angles further induce the formation of HLCT states in these molecules, which is verified by DFT simulation and solvatochromic experiments. We further explore their potentials in OL *via* ASE measurements, where **PT2** showed an optimal threshold of 20 μJ/cm^2. In summary, we presented a green and low-cost method to suppress ACQ in organic semiconductors and induces HLCT states at the same time, offering a solution for the scalable material production for next-generation electroluminescence devices.

Acknowledgements

The authors would also like to acknowledge the financial support from the Clean Energy Institute, NSF Center for Selective C– H Functionalization (CHE-1700982) and a Materials Research Science and Engineering Center (DMR-1719797). Y.H. and D.S.G. acknowledge ONR N00014-17-1-2201 for supporting experiments facilitating characterization of the chromophores. Y.H. thanks the Data Intensive Research Enabling Clean Technology (DIRECT) NSF National Research Traineeship (DGE-1633216) for support. The X-Ray facility is supported by NSF Grant 0840520.

Conflicts of interest

There are no conflicts to declare.

Notes and references

1 a) J. B. Birks, *Photophysics of Aromatic Molecules*, Wiley, London, 1970; b) Y. Hong, J. W. Y. Lam and B. Z. Tang, *Chem. Soc. Rev.*, **2011**, *40*, 5361.
2 Z. Zhao, S. Gao, X. Zheng, P. Zhang, W. Wu, R. T. K. Kwok, Y. Xiong, N. L. C. Leung, Y. Chen, X. Gao, J. W. Y. Lam and B. Z. Tang, *Adv. Funct. Mater*., **2018**, *28*, 1705609.
3 A. J. C. Kuehne and M. C. Gather, *Chem. Rev*., **2016**, *116*, 12823.
4 a) S. Li and D. Yan, *Adv. Opt. Mater*., **2018**, *6*, 1800445; b) S. Li, Y. Lin and D. Yan, *J. Mater. Chem. C*, **2016**, *4*, 2527.
5 a) R. Jakubiak, Z. Bao and L. Rothberg, *Synth. Met.*, **2000**, *114*, 61; b) S. Rehm, V. Stepanenko, X. Zhang, T. H. Rehm and F. Würthner, *Chem. Eur. J*., **2010**, *16*, 3372; c) J. Mei, N. L. C. Leung, R. T. K. Kwok, J. W. Y. Lam and B. Z. Tang, *Chem. Rev*., **2015**, *115*, 11718.
6 Y. Diao, L. Shaw, Z. Bao and S. C. B. Mannsfeld, *Energy Environ. Sci.*, **2014**, *7*, 2145.
7 a) W.-Y. Lai, R. Zhu, Q.-L. Fan, L.-T. Hou, Y. Cao and W. Huang, *Macromolecules*, **2006**, *39*, 3707; b) P. A. Levermore, R. Xia, W. Lai, X. H. Wang, W. Huang and D. D. C. Bradley, *J. Phys. D: Appl. Phys.*, **2007**, *40*, 1896; c) W.-Y. Lai, R. Xia, D. D. C. Bradley and W. Huang, *Chem. Eur. J*., **2010**, *16*, 8471.
8 a) J. Wang, Y. Zhao, C. Dou, H. Sun, P. Xu, K. Ye, J. Zhang, S. Jiang, F. Li and Y. Wang, *J. Phys. Chem. B*, **2007**, *111*, 5082; b) S. Hecht and J. M. J. Fréchet, *Angew. Chem. Int. Ed*., **2001**, *40*, 74.
9 Á. Molnár, *Chem. Rev*., **2011**, *111*, 2251.
10 a) K. Okamoto, J. Zhang, J. B. Housekeeper, S. R. Marder and C. K. Luscombe, *Macromolecules*, **2013**, *46*, 7565; b) T. Bura, J. T. Blaskovits and M. Leclerc, *J. Am. Chem. Soc.*, **2016**, *138*, 10056; c) Y. Huang and C. L. Luscombe, *Chem. Rec*., **2019**, *19*, 1.
11 Y. Huang, D. L. Elder, A. L. Kwiram, S. A. Jenekhe, A. K. Y. Jen, L. R. Dalton and C. K. Luscombe, *Adv. Mater*., **2019**, 1904239.
12 N. A. Strotman, H. R. Chobanian, Y. Guo, J. He and J. E. Wilson, *Org. Lett*., **2010**, *12*, 3578.
13 J. S. Barber, S. Scales, M. Tran-Dubé, F. Wang, N. W. Sach, L. Bernier, M. R. Collins, J. Zhu, I. J. McAlpine and R. L. Patman, *Org. Lett*., **2019**, *21*, 5689.
14 S. Vidyacharan, B. T. Ramanjaneyulu, S. Jang and D.-P. Kim, *ChemSusChem,* **2019**, *12*, 2581.
15 S. I. Gorelsky, D. Lapointe and K. Fagnou, *J. Am. Chem. Soc*., **2008**, *130*, 10848.
16 B. Liégault, I. Petrov, S. I. Gorelsky and K. Fagnou, *J. Org. Chem.,*

2010, *75*, 1047.
17 a) F. Würthner, C. R. Saha-Möller, B. Fimmel, S. Ogi, P. Leowanawat and D. Schmidt, *Chem. Rev.*, **2016**, *116*, 962; b) Y. Huang, N. Zheng, Z. Wang, L. Ying, F. Huang and Y. Cao, *Chem. Commun.,* **2017**, *53*, 1997; c) Y. Huang, W. Xu, C. Zhou, W. Zhong, R. Xie, X. Gong, L. Ying, F. Huang and Y. Cao, *J. Polym. Sci., Part A: Polym. Chem.*, **2016**, *54*, 2119
18 T. M. Figueira-Duarte, P. G. Del Rosso, R. Trattnig, S. Sax, E. J. W. List and K. Mullen, *Adv. Mater*., **2010**, *22*, 990.
19 a) D. Yan and D. G. Evans, *Mater. Horiz.,* **2014**, *1*, 46; b) F. Würthner, C. R. Saha-Möller, B. Fimmel, S. Ogi, P. Leowanawat and D. Schmidt, *Chem. Rev*., **2016**, *116*, 962; c) J. Gierschner, S. Varghese, and S. Y. Park, *Adv. Optical Mater*., **2016**, *4*, 348.
20 a) H. Kaji, H. Suzuki, T. Fukushima, K. Shizu, K. Suzuki, S. Kubo, T. Komino, H. Oiwa, F. Suzuki, A. Wakamiya, Y. Murata and C. Adachi, *Nat. Comm*., **2015**, *6*, 8476; b) G. Grancini, M. Maiuri, D. Fazzi, A. Petrozza, H-J. Egelhaaf, D. Brida, G. Cerullo and G. Lanzani, *Nat. Mater*., **2013**, *12*, 29; c) X. Zhang, M. W. Cooper, Y. Zhang, C. Fuentes-Hernandez, S. Barlow, S. R. Marder and B. Kippelen, *ACS Appl. Mater. Interfaces,* **2019**, *11*, 12693; d) K. Lin, B. Xie, Z. Wang, R. Xie, Y. Huang, C. Duan, F. Huang and Y. Cao, *Org. Electron*., **2018**, *52*, 42.
21 a) W. Li, D. Liu, F. Shen, D. Ma, Z. Wang, T. Feng, Y. Xu, B. Yang and Y. Ma, *Adv. Funct. Mater*., **2012**, *22*, 2797; b) W. Li, Y. Pan, R. Xiao, Q. Peng, S. Zhang, D. Ma, F. Li, F. Shen, Y. Wang, B. Yang and Y. Ma, *Adv. Funct. Mater*., **2014**, *24*, 1609; c) W. Li, Y. Pan, L. Yao, H. Liu, S. Zhang, C. Wang, F. Shen, P. Lu, B. Yang and Y. Ma, *Adv. Optical Mater*., **2014**, *2*, 892
22 a) A. Köhn and C. Hättig, *J. Am. Chem. Soc.*, **2004**, *126*, 7399; b) C. J. Jödicke and H. P. Lüthi, *J. Am. Chem. Soc.*, **2003**, *125*, 252; c) A. Chakraborty, S. Kar and N. Guchhait, *Chem. Phys.*, **2006**, *324*, 733.
23 M. D. McGehee and A. J. Heeger, *Adv. Mater.*, **2000**, *12*, 1665.
24 a) J. Zhou, X. Wan, Y. Liu, Y. Zuo, Z. Li, G. He, G. Long, W. Ni, C. Li, X. Su and Y. Chen, *J. Am. Chem. Soc.*, **2012**, *134*, 16345; b) B. Walker, C. Kim and T.-Q. Nguyen, *Chem. Mater*., **2011**, *23*, 470.
25 a) M. Anni, A. Perulli and G. Monti, *J. Appl. Phys.*, **2012**, *111*, 093109; b) D.-H. Kim, A. S. D. Sandanayaka, L. Zhao, D. Pitrat, J. C. Mulatier, T. Matsushima, C. Andraud, J. C. Ribierre and C. Adachi, *Appl. Phys. Lett.*, **2017**, *110*, 023303.
26 M. Campoy-Quiles, G. Heliotis, R. Xia, M. Ariu, M. Pintani, P. Etchegoin and D. D. C. Bradley, *Adv. Funct. Mater*., **2005**, *15*, 925.
27 M. E. Ziffer, S. B. Jo, Y. Liu, H. Zhong, J. C. Mohammed, J. S. Harrison, A. K.-Y. Jen and D. S. Ginger, *J. Phys. Chem. C*, **2018**, *122*, 18860.